Physics Letters B 741 (2015) 272–275

Contents lists available at ScienceDirect

Physics Letters B

www.elsevier.com/locate/physletb

Position resolution limits in pure noble gaseous detectors for X-ray energies from 1 to 60 keV

C.D.R. Azevedo [a,*], S. Biagi [b], R. Veenhof [b,c], P.M. Correia [a], A.L.M. Silva [a], L.F.N.D. Carramate [a], J.F.C.A. Veloso [a]

[a] I3N – Physics Department, University of Aveiro, 3810-193 Aveiro, Portugal
[b] Uludağ University, Faculty of Arts and Sciences, Physics Department, Bursa, Turkey
[c] RD51 Collaboration, CERN, CH-1211 Geneva 23, Switzerland

ARTICLE INFO

Article history:
Received 11 September 2014
Received in revised form 24 December 2014
Accepted 26 December 2014
Available online 5 January 2015
Editor: W. Haxton

Keywords:
Gaseous detectors
Intrinsic position resolution
X-rays
Noble gas

ABSTRACT

The calculated position resolutions for X-ray photons (1–60 keV) in pure noble gases at atmospheric pressure are presented. In this work we show the influence of the atomic shells and the detector dimensions on the intrinsic position resolution of the used noble gas. The calculated results were obtained by using a new software tool, Degrad, and compared to the available experimental data.

1. Introduction

Since the invention of the Multi-Wire Proportional Chamber (MWPC) by G. Charpack in 1968, noble gases have been exhaustively used as a radiation detection medium. The discovery of new particles like J/ψ meson by Ting and Richter or the W and Z bosons by Rubia have been done in experiments using noble gas radiation detection [1]. Nowadays, the use of noble gases is still in the front line for new discoveries as, for example, the 0-$\nu\beta\beta$ in NEXT or the search for dark matter [2–4]. In addition, their use in radiation detectors has crossed the field of HEP experiments to find applications in medical imaging [5] or homeland security [6].

The position resolution is an essential capability of gas-filled radiation detectors that has been extensively explored. A long bibliography on position sensitive gaseous detectors is already available, namely in particle tracking devices [1,7]. However the discussion of the position resolution is generally centred in the device itself without fully exploring the gas influence.

X-rays are indirect ionizing radiation, providing different physics processes than ionizing particles. In this case, the position resolution depends not only on the photoelectron range [8] but also on the energy loss mechanisms during the photoelectron drift and thermalization in the gas. In gaseous detectors the interaction position of the incoming photons is usually obtained through the centre-of-gravity of the produced spatial charge distribution, thus, the atom de-excitation processes like Auger emission, Coster–Kronig or Shake-off, will govern the charge spread process over the photoelectron range.

Another process that can contribute to the position resolution degradation is the fluorescence photon interaction within the detector volume. The absorption of the fluorescence photon will shift the charge distribution centroid and thus, the detected position, contributing to a broadening of the position distribution. At low energies elastic Rayleigh scattering of the fluorescence photon can also contribute to the resolution and is accounted for in the simulation.

2. The toolkit

The position resolutions here presented were calculated for different gases as function of the X-ray photon energy by using a simulation program based on Monte Carlo simulation: Degrad [9].

Degrad is a new software tool developed by S. Biagi, which is an accurate Auger cascade model for interaction of photons

* Corresponding author.
E-mail address: cdazevedo@ua.pt (C.D.R. Azevedo).

http://dx.doi.org/10.1016/j.physletb.2014.12.054

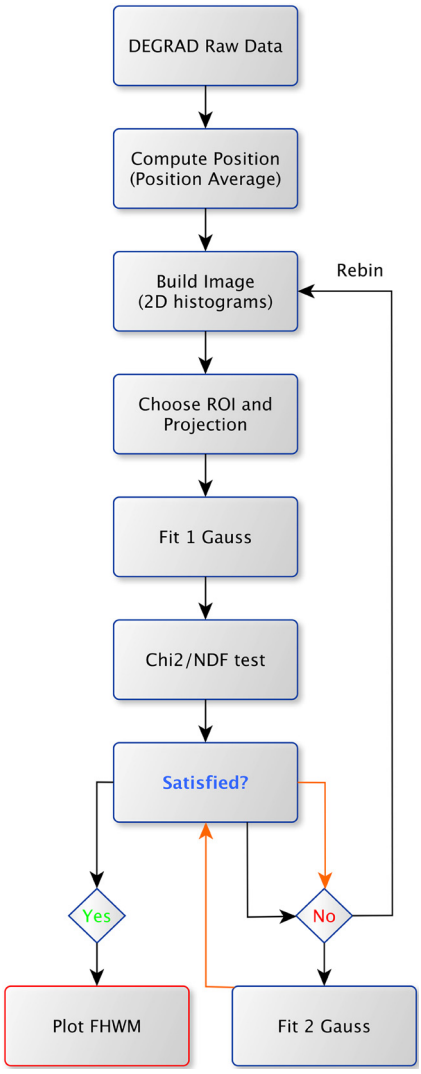

Fig. 1. Flow chart describing the analysis chain.

and particles with gas mixtures in electric and magnetic fields. The software simulates automatically, for X-rays, the shell absorption by photoelectric effect or Compton scattering and the subsequent Auger, Coster–Kronig, Shake-off and fluorescence emission. Bremsstrahlung emissions by secondary electrons are also included [10]. The program also calculates the number of ionizations and excitations produced in the gas medium after electron energy thermalization and returns the Fano factors for both.

The individual events can be output, i.e., the position and time of thermalization of each electron, which means that a detailed analysis can be performed with other detector simulation programs.

Preliminary tests on the noble gases give Fano factors with an accuracy better than 3% up to 20 keV [1].

3. Analysis chain

The analysis chain is described in the flow chart of Fig. 1. The first step is to convert the Degrad data file into a ROOT file [11], i.e., the software used for the analysis process.

The analysis is performed event by event, i.e., each single X-ray photon interaction in the gas, being the interaction position calculated through the center-of-gravity of all the electrons thermalized positions.

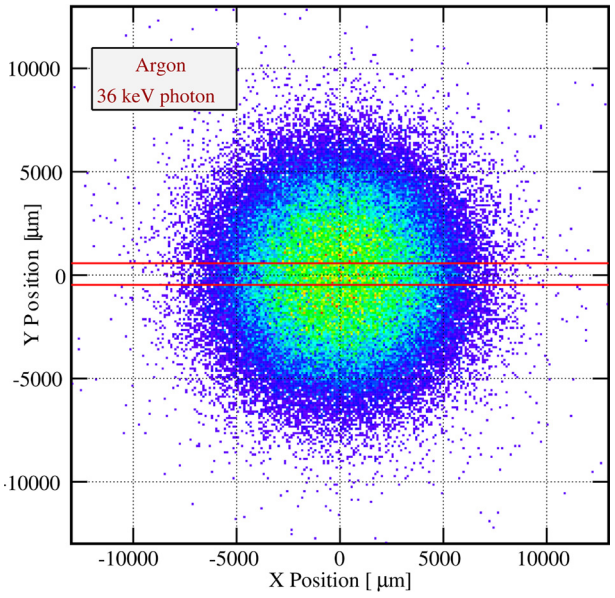

Fig. 2. Example of a reconstructed image for 36 keV photons in argon.

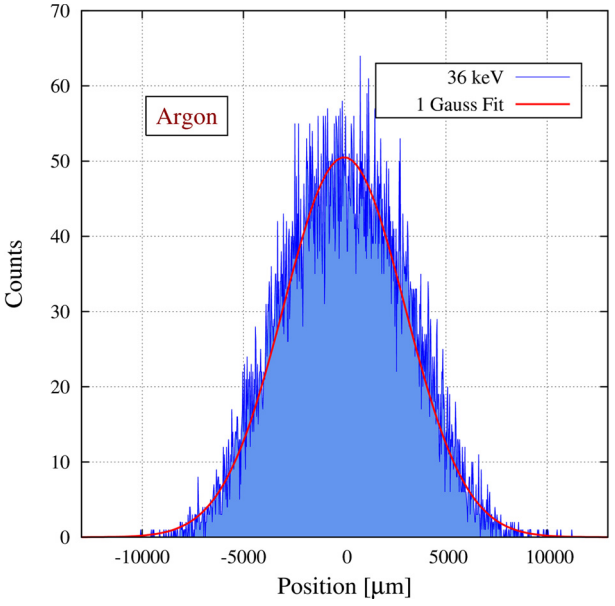

Fig. 3. The projection of the events selected on the previous image.

For each considered photon energy an image is reconstructed by making the 2D histogram of the calculated positions (X and Y), as presented in Fig. 2. A region-of-interest was defined as 4% of the histogram range, centred in the central bin (represented between the horizontal lines in Fig. 2), followed by its projection (cumulative sum in the X direction).

The position resolution was achieved through the FWHM of a fitted Gaussian function to the projected data, Fig. 3, similarly to the Line Spread Function (LSF) method [12].

In order to evaluate the fit quality a χ^2/NDF test was applied. If the result is considered satisfactory, i.e., $1 < \chi^2/\text{NDF} < 1.5$, the analysis is finished. In the case that the results are not well described by a one Gaussian model a two Gaussian model is fitted, Fig. 4. This occurs, generally, for energies right after the atomic shells absorptions, where the interaction probability on both shells is similar. In this case, the position resolution was considered to be the FWHM of the Gaussian with greatest amplitude. Although,

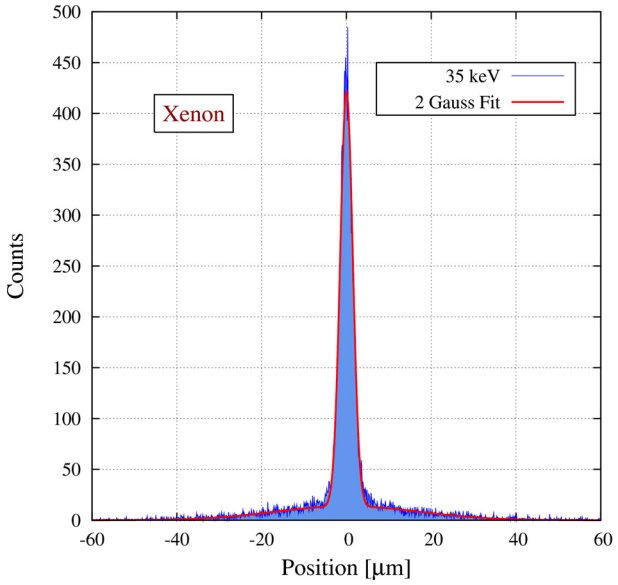

Fig. 4. Example of a 2 Gaussian fit model to a energy right after the K absorption shell in xenon.

if none of the models produce good fit results a rebin of the initial 2D histogram was done, followed again by the described analysis.

4. Results

In this work we have made calculations for pure noble gases (helium, neon, argon, krypton and xenon) for X-ray photons with energies ranging from 1 to 60 keV in 1 keV step. The gas was considered to be at 760 Torr and 20 °C. All the photons interact in the (0, 0, 0) position where a 1 kV/cm electric field was set in the direction parallel to the incoming photons. 110,000 events were simulated for each condition, i.e. gas and photon energy combination. In order to decrease the calculations time, the electrons were considered thermalized when their energy falls to 1 eV below the lowest excitation energy of the gas: He = 19.8 eV, Ne = 16.6 eV, Ar = 11.6 eV, Kr = 9.9 eV and Xe = 8.3 eV [13,14].

By discriminating the thermalized electron's positions we can consider two different analysis: an analysis that we call *"infinite"*, where all electrons are accepted; and a finite example denominated as *"Detector"* where just the electrons with thermalized positions inside a volume ($10 \times 10 \times 1$ cm^3) are considered, thus simulating a detector active volume.

The results for an *"infinite"* geometry are shown in Fig. 5. As expected helium is the gas that presents the worst performance followed by neon, argon, Kr and Xe (enumerated by descending order of the position resolution value). For Ar, Kr and Xe there is an evident improvement in the position resolution after the respective L and K shells ($K_{Ar} \approx 3$ keV, $K_{Kr} \approx 14$ keV, $K_{Xe} \approx 35$ keV [15]). This benefit is due to the contribution of the greater binding energy of the inner shells, resulting in lower energetic photoelectrons and thus, in a lower charge spread. On the other hand, due to the atom rearrangement, a characteristic fluorescence photon is emitted and can be absorbed somewhere in the active volume producing a new primary electron cloud that will shift the initial position detection, masking the benefit of the photoelectron energy reduction. The fluorescence photon interaction point will depend on the photon energy (for example: $Ar_{K_\alpha} \approx 3$ keV, $Kr_{K_\alpha} \approx 13$ keV and $Xe_{K_\alpha} \approx 30$ keV [15]) and obviously on the gas density.

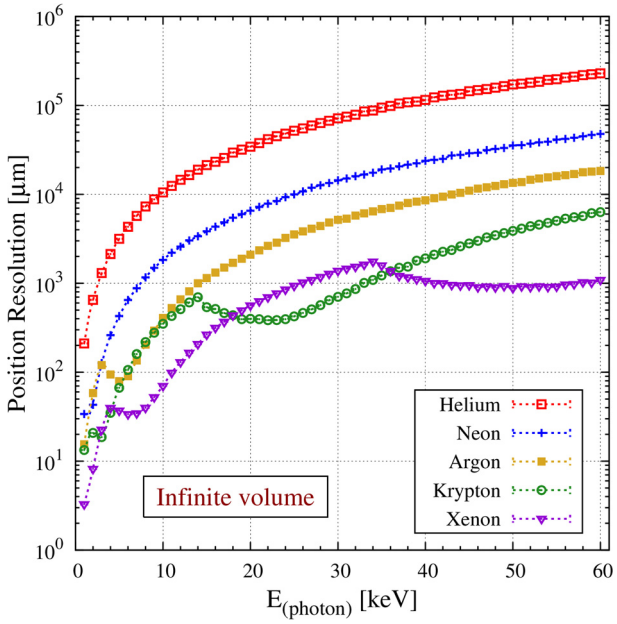

Fig. 5. Position resolution as a function of the photon energy for an "infinite" geometry.

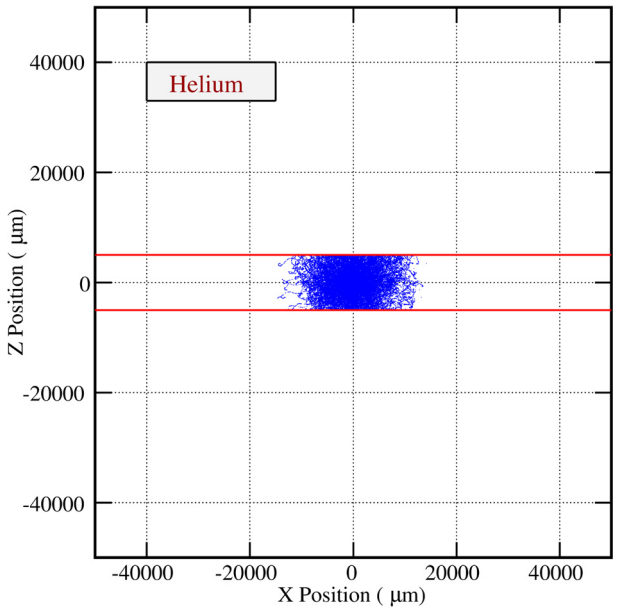

Fig. 6. Image of the thermalized electron positions produced by a 10 keV photon in helium.

When a finite geometry is used, the fluorescence photons interaction is limited to the detector active volume and, in the case of more energetic fluorescence photons (Kr and Xe K fluorescence) the interaction probability is lower contributing to the escape peaks. In such case (Fig. 7), the position resolution will be dominated by the photoelectron range, contributing to a better position resolution when compared to the case of "infinite" geometry. This effect is less pronounced on the Kr and Xe L shells ($L_{Kr} \approx 2$ keV and $L_{Xe} \approx 5$ keV [15]) and on the Ar K shell, where the fluorescence photons are less energetic ($Kr_{L_\alpha} \approx 1.6$ keV and $Xe_{L_\alpha} \approx 4$ keV [15]) and the interaction probability with the gas is not negligible. In Fig. 7 the experimental values from [16] are also shown. In general we can observe that Degrad reproduces the experimental data with good accuracy, except for the argon when the photon

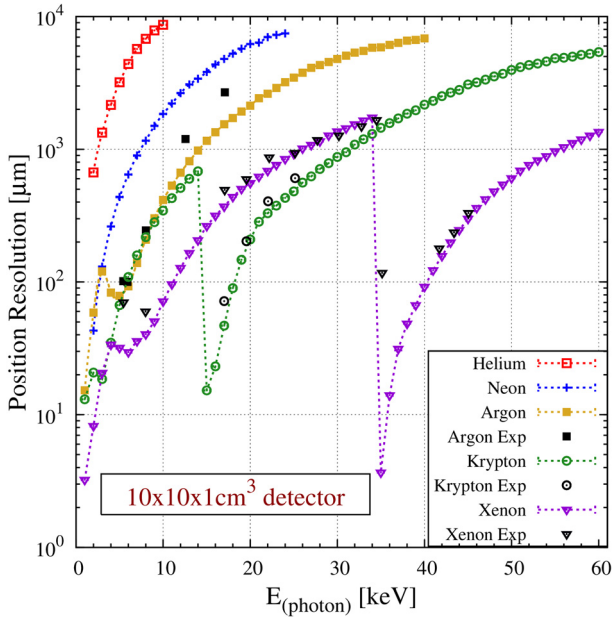

Fig. 7. Position resolution as a function of the photon energy for a $10 \times 10 \times 1$ cm^3 detector.

energy is bigger than 10 keV and for energy values just after the Xe K and L shells, where we are convinced that the experimental data is influenced by the intrinsic position resolution of the used detector [16].

In the detector limited volume case, we just present the position resolution values until 10 mm, which corresponds to the lowest detector dimension. When the spatial distribution of the primary electrons approaches this value, the electrons start to be lost to the detectors walls, Fig. 6. In this situation a huge error is introduced in the position calculation and to continue with the calculations has no more physical interest.

A very interesting aspect is that, for the range 14–34 keV, Kr presents a better position resolution than Xe, making Kr the perfect choice for applications requiring photon detection on that range.

5. Conclusions

We have studied the X-ray detection, from 1 to 60 keV, in pure noble gas detectors in terms of position resolution. An improvement of the position resolution when the X-ray photons have higher energy than the gas atomic shell energy was verified. The position resolution dependence with the energy and with the atomic number was observed. An exception was verified for krypton in the range from 14–34 keV where it presents better performance than xenon. Finally, the influence of the detector geometry on the position resolution was also discussed.

Acknowledgements

This work was partially supported by projects CERN/FP/123604/2011 and PTDC/FIS/110925/2009 through FEDER, COMPETE and FCT (Lisbon) programs. C.D.R. Azevedo was supported by PostDoctoral grant from FCT (Lisbon) SFRH/BPD/79163/2011. P.M. Correia and L.F.N.D. Carramate were supported by the FCT (Lisbon) scholarships BD/52330/2013 and SFRH/BD/71429/2010, respectively. A.L.M. Silva was supported by QREN programme Mais Centro, FEDER and COMPETE, through project CENTRO-07-ST24-FEDER-002030. The research was done within the CERN RD51 Collaboration.

References

[1] E. Aprile, et al., Noble Gas Detectors, Wiley–VCH, 2006.
[2] D. Nygren, Simultaneous 0-$\nu\beta\beta$ decay & WIMP dark matter searches, http://agenda.albanova.se/materialDisplay.py?materialId=slides&confId=4789.
[3] V.M. Gehman, et al., J. Instrum. 8 (2013) C10001, http://dx.doi.org/10.1088/1748-0221/8/10/C10001.
[4] J.J. Gomez Cadenas, et al., Adv. High Energy Phys. 2014 (2014), http://dx.doi.org/10.1155/2014/907067.
[5] M.N. Wernick, et al., Emission Tomography: The Fundamentals of PET and SPECT, Elsevier Academic Press, 2004.
[6] K. Gnanvo, et al., Nucl. Instrum. Methods Phys. Res., Sect. A, Accel. Spectrom. Detect. Assoc. Equip. 652 (2011) 16–20, http://dx.doi.org/10.1016/j.nima.2011.01.163.
[7] G.F. Knoll, Radiation Detection and Measurement, 3rd edition, John Wiley & Sons, New York, 2000.
[8] G.C. Smith, et al., IEEE Trans. Nucl. Sci. 31 (1) (1984) 111–115, http://dx.doi.org/10.1109/TNS.1984.4333221.
[9] S. Biagi, Degrad, http://consult.cern.ch/writeup/magboltz/.
[10] S. Biagi, Program DEGRAD an accurate auger cascade model for interaction of photons and particles with gas mixtures in electric and magnetic fields, http://indico.cern.ch/event/245535/session/5/contribution/14/material/slides/, 2013.
[11] ROOT — a data analysis framework, 2014, http://root.cern.ch/drupal/.
[12] S.W. Smith, Special Imaging Techniques, 2nd edition, Elsevier Science, 1999, pp. 423–429, Ch. 25.
[13] S. Biagi, Magboltz, http://consult.cern.ch/writeup/magboltz/.
[14] C.A.B. Oliveira, Monte Carlo study of electroluminescence in gaseous detectors, Ph.D. thesis, Universidade de Aveiro, 2011, http://hdl.handle.net/10773/7346.
[15] C. Segre, Periodic table, http://www.csrri.iit.edu/periodic-table.html.
[16] G. Smith, Lecture on gaseous detectors for science & discussion, https://indico.cern.ch/event/179611/session/4/contribution/0/material/slides/0.pdf.